Supporting Information

Intracellular Monitoring of NADH Release from Mitochondria Using a Single Functionalized Nanowire Electrode

*Hong Jiang, Yu-Ting Qi, Wen-Tao Wu, Ming-Yong Wen, Yan-Ling Liu and Wei-Hua Huang**

College of Chemistry and Molecular Sciences, Wuhan University, Wuhan 430072, China

E-mail: whhuang@whu.edu.cn

Table of Contents

Supporting Figures

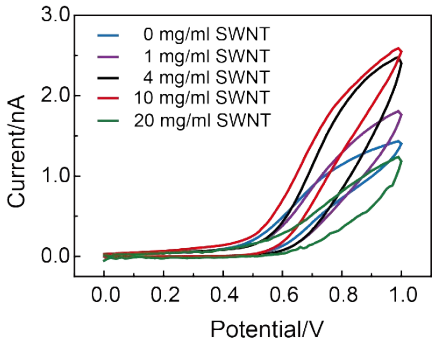

Figure S1. Optimization of electrochemical properties of CNTs@PEDOT-NWE by changing the CNTs/PEDOT ratio. Cyclic voltammograms of different CNTs@PEDOT-NWEs in 2 mM NADH; scan rate was 0.1 V s^{-1}. The length and diameter of NWEs were precisely controlled to ensure the similar electroactive area of each CNTs@PEDOT-NWE.

In this experiment, we added different amounts of SWNTs to the same concentration of PEDOT: PSS solutions (1% PEDOT: PSS solution with 5% DMSO), and the concentration of SWCNTs are 0, 1, 4, 10 and 20 mg ml^{-1}, respectively. The Cyclic voltammograms showed that the current intensities were increased with increasing SWCNTs concentration (0, 1, 4, 10 mg ml^{-1}). This may result from the higher concentrations of SWCNTs which was thought to increase the electrical conductivity and the electroactive surface area of the CNTs@PEDOT-NWE. However, further increase the concentration of SWCNTs (20 mg ml^{-1}) resulted in a decrease of the current intensity. The possible reason was that excessive SWCNTs adsorbed on the electrode surface made the electrode surface negatively charged, preventing the accumulation of negatively charged NADH on the electrode surface. Therefore, the 10 mg ml^{-1} was selected as the optimal concentration of CNTs to provide the best electrochemical properties.

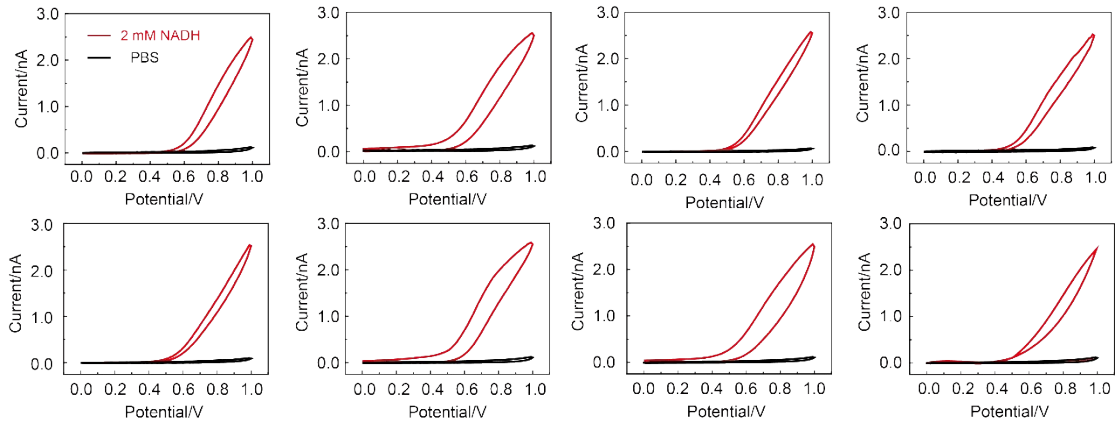

Figure S2. Cyclic voltammograms of 8 CNTs@PEDOT-NWEs in the absence (black curves) and presence (red curves) of 2 mM NADH. Scan rate was 0.1 V s^{-1}.

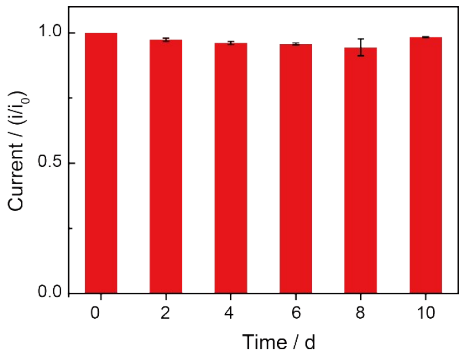

Figure S3. Stability test of the CNTs@PEDOT-NWE by successive detection of 2 mM NADH solution for 10 days. (means and SEM, n = 3)

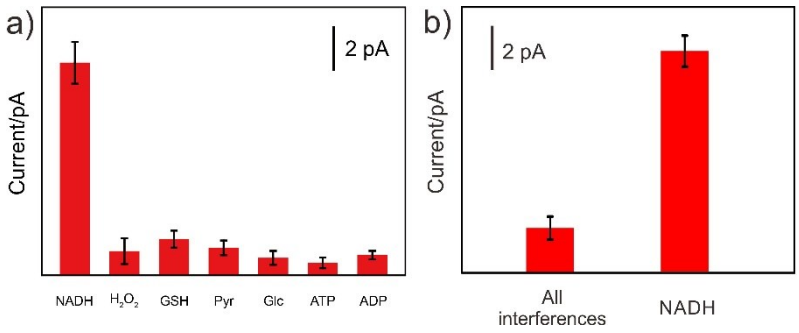

Figure S4. Selective profile of the CNTs@PEDOT-NWE to interferences. a) Interferences present separately. b) All the interferences present at the same time. The concentration of each component was 50 μM. (means and SEM, n = 3)

Resveratrol and paclitaxel can regulate the intracellular metabolism and induce the variation of concentration levels of relevant biomolecule such as H_2O_2, glutathione (GSH), pyruvic acid (Pyr), glucose (Glc), ATP and ADP, et al.[1] Hence, H_2O_2, GSH, Pyr, Glc, ATP and ADP were chosen as interferences to investigate the selectivity of CNTs@PEDOT-NWE toward detection of NADH.

The positively charged PEDOT contributes to the accumulation of negatively charged analyte and thus enhanced analytical performance of NADH. Given that Pyr, Glc, ADP and ATP have poor electrochemical activity, H_2O_2 is electrically neutral under physiological conditions, and GSH requires a larger overpotential,[2] the current of NADH on the electrode surface was 6 ~ 17 times higher than that of interferences. And when all the interferences present at the same time, the current of NADH on the electrode surface was 5 times higher than that of the sum of all interferents. Further considering that the intracellular H_2O_2 concentration is usually lower than 10 nM and the intracellular concentration of GSH, Pyr, Glc, ATP and ADP are on the same order of magnitude with NADH (~ μM range),[3-10] these results showed that the CNTs@PEDOT-NWE possessed the desired selectivity to monitor NADH fluctuations caused by abnormal cell metabolism inside single living cells.

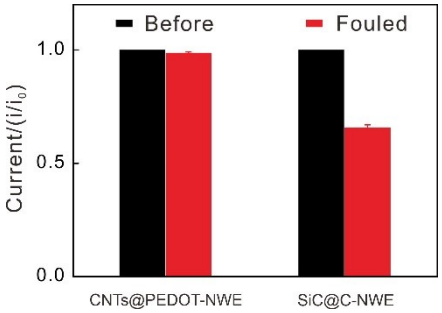

Figure S5. The antifouling performance of CNTs@PEDOT-NWE. CVs in $Ru(NH_3)_6^{3+}$ on the CNTs@PEDOT-NWE and SiC@C-NWE before and after passivation by culture medium for 3h. (means and SEM, n = 4)

The response of the CNTs@PEDOT-NWE could maintain over 98.7 ± 0.4% of the originals after passivation treatment, while the response of the SiC@C-NWE decreased by 34.2 ± 0.4 %. The results demonstrated that the CNTs@PEDOT-NWE has a good antifouling performance.

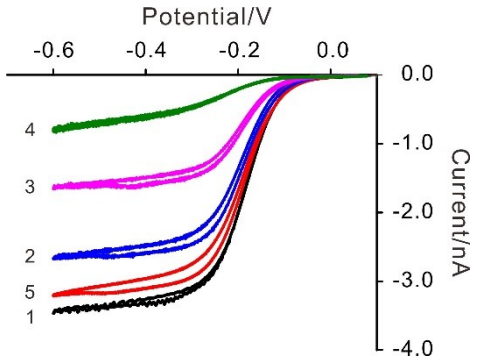

Figure S6. CVs recorded at a CNTs@PEDOT-NWE at different positions from outside the cell to inside the cell when 1 mM $Ru(NH_3)_6^{3+}$ was added to the cell bath. Curve 1: outside the cell; curve 2: approximately 25% inside; curve 3: approximately 50% inside; curve 4: approximately 75% inside; curve 5: after withdrawal out of the cell.

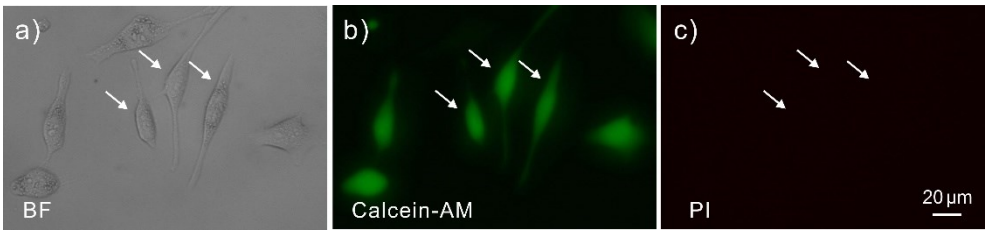

Figure S7. MCF-7 cells after CNTs@PEDOT-NWE insertion (indicated by arrows) under a) bright-field (BF) and fluorescence imaging after staining with b) Calcein-AM and c) propidium iodide (PI).

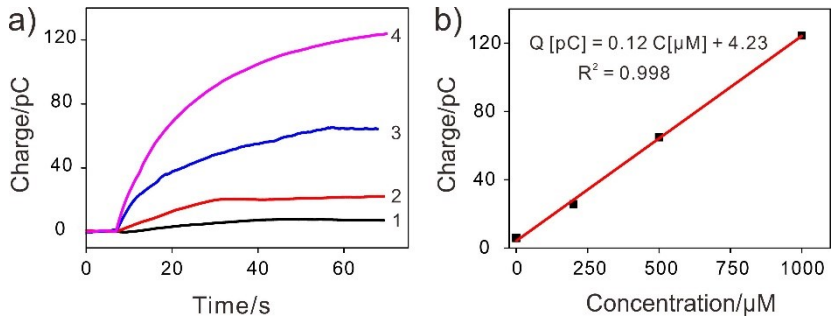

Figure S8. Charge traces obtained from MCF-7 cells pre-loaded with 0 (curve 1), 200 (curve 2), 500 (curve 3), and 1000 (curve 4) μM NADH a) and the corresponding calibration curves b).

According to the equation $x = \sqrt{Dt}$ (where x is the diffusion distance, D is the diffusion coefficient and t is the diffusion time), the diffusion distance could reach 150 μm in the whole detection time (100 s), which was greatly larger than the size of single cells. Therefore, we think that almost all the released NADH molecules could diffuse to the nanoelectrode for detection.

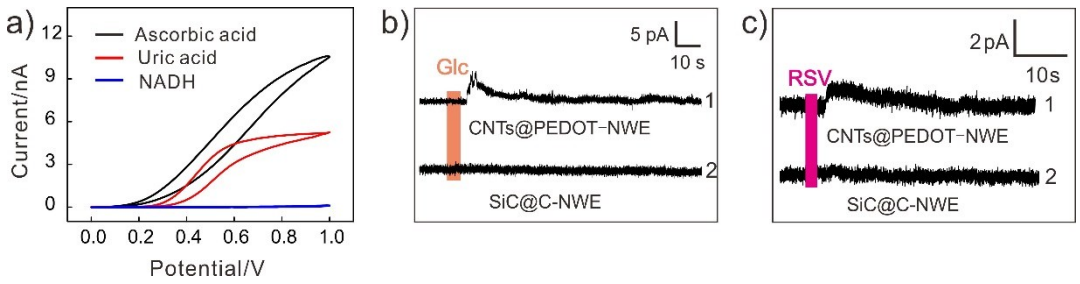

Figure S9. a) CVs recorded with 2 mM ascorbic acid, uric acid and NADH at SiC@C-NWE. b) Amperometric traces obtained from glucose-induced and c) RSV-induced NADH release with a SiC@C-NWE (curve 2) and CNTs@PEDOT-NWE (curve 1).

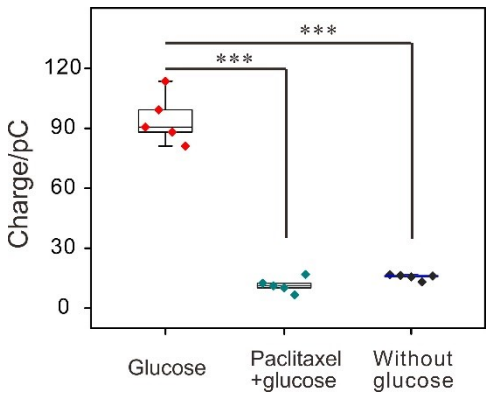

Figure S10. The charge statistics of MCF-7 cells with 1 mM glucose injection, 20 μM paclitaxel incubation and 1 mM glucose injection, or without glucose injection. The charge of NADH released under the three situations are 94.6 ± 5.6 pC, 11.5 ± 1.6 pC and 15.7 ± 0.6 pC, respectively. (means and SEM, n = 5, ***P < 0.001)

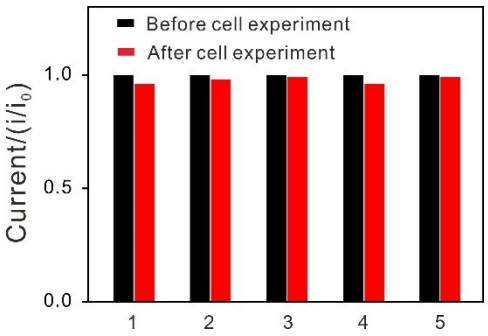

Figure S11. Electrochemical responses of 5 CNTs@PEDOT-NWEs to 2 mM NADH before and after cell experiment.

Table S1. Materials and performance characteristics of NADH electrochemical sensors in PBS solution.

Electrode	Modifying materials	LOD (μM)	Reference
SPE	Meldola Blue	2.5	11
GCE	Thionine-CNTs/Nafion	1.0	12
GCE	Acid-treated CNTs	2.0	13
GCE	Fe_3O_4/MWCNTs	5.0	14
RDE	N-CNT	1.1	15
GCE	GN-AuNRs	6	16
GCE	PEDOT	5.3	17
GCE	CNT-CHIT	3	18
SiC@C-NWE	SWNTs@PEDOT	0.7	This work

LOD, limit of detection. SPE, screen-printed graphite. GCE, glassy carbon electrode. RDE, pine rotating disk electrode. CHIT, chitosan. GN, graphene. AuNRs, Au nanorods. CNTs, carbon nanotubes. MWCNTs, multiwalled carbon nanotubes.

References

[1] J. Mikuła-Pietrasik, A. Witucka, M. Pakuła, P. Uruski, B. Begier-Krasińska, A. Niklas, A. Tykarski, K. Książek, *Cell. Mol. Life Sci.* 2019, **76**, 681-697.

[2] N. Pereira-Rodrigues, R. Cofré, J. H. Zagal, F. Bedioui, *Bioelectrochemistry* 2007, **70**, 147-154.

[3] V. Guarino, W. Oldham, J. Loscalzo, Y. Y. Zhang, *Sci. Rep.* 2019, **9**, 19568-19576.

[4] A. Fulati, S. Usman Ali, M. Asif, N. Hassan Alvi, M. Willander, C. Brannmark, P. Stralfors, S. Borjesson, F. Elinder, B. Danielsson, *Sens. Actuators, B* 2010, **150**, 673-680.

[5] S. P. Williams, A. M. Fulton, K. M. Brindle, *Biochemistry* 1993, **32**, 4895-4902.

[6] X. Hun, Y. X. Li, S. Y. Wang, Y. Li, J. K. Zhao, H. Zhang, X. L. Luo, *Biosens. Bioelectron.* 2018, **112**, 93-99.

[7] M. Bonora, S. Patergnani, A. Rimessi, E. D. Marchi, J. M. Suski, A. Bononi, C. Giorgi, S. Marchi, S. Missiroli, F. Poletti, M. R. Wieckowski, P. Pinton, *Purinergic Signalling* 2012, **8**, 343-357.

[8] Y. Zhao, J. Jin, Q. Hu, H. Zhou, J. Yi, Z. Yu, L. Xu, X. Wang, Y. Yang, J. Loscalzo, *Cell Metab.* 2011, **14**, 555-566.

[9] W. Ying, *Antioxid. Redox Signaling* 2008, **10**, 179-206.

[10] W. Xie, A. Xu, E. S. Yeung, *Anal. Chem*. 2009, **81**, 1280-1284.

[11] A. Vasilescu, S. Andreescu, C. Bala, S. C. Litescu, T. Noguer, J. Marty, *Biosens. Bioelectron.* 2003, **18**, 781-790.

[12] M. Huang, H. Jiang, J. Zhai, B. Liu, S. Dong, *Talanta* 2007, **74**, 132-139.

[13] M. Wooten, W. Gorski, *Anal. Chem.* 2010, **82**, 1299-1304.

[14] H. Teymourian, A. Salimi, R. Hallaj, *Biosens. Bioelectron.* 2012, **33**, 60-68.

[15] J. M. Goran, C. A. Favela, K. J. Stevenson, *Anal. Chem.* 2013, **85**, 9135-9141.

[16] L. Li, H. Lu, L. Deng, *Talanta* 2013, **113**, 1-6.

[17] L. Meng, A. P. F. Turner, W. C. Mak, *Biosens. Bioelectron.* 2018, **120**, 115-121.

[18] M. Zhang, A. Smith, W. Gorski, *Anal. Chem.* 2004, **76**, 5045-5050.